

Most spin-1/2 transition-metal ions do have single ion anisotropy

Jia Liu¹, Hyun-Joo Koo², Hongjun Xiang^{3,*}, Reinhard K. Kremer⁴ and Myung-Hwan Whangbo^{1,*}

¹ Department of Chemistry, North Carolina State University, Raleigh, North Carolina 27695, USA

² Department of Chemistry and Research Institute for Basic Sciences, Kyung Hee University, Seoul 130-701, Republic of Korea

³ Key Laboratory of Computational Physical Sciences (Ministry of Education), State Key Laboratory of Surface Physics, and Department of Physics, Fudan University, Shanghai 200433, People's Republic of China

⁴ Max-Planck-Institut für Festkörperforschung, Heisenbergstrasse 1, D-70569 Stuttgart, Germany

PACS Numbers: 71.70.Ej, 75.10.Dg, 75.25.-j

Abstract

The cause for the preferred spin orientation in magnetic systems containing spin-1/2 transition-metal ions was explored by studying the origin of the easy-plane anisotropy of the spin-1/2 Cu^{2+} ions in $\text{CuCl}_2 \cdot 2\text{H}_2\text{O}$, LiCuVO_4 , CuCl_2 and CuBr_2 on the basis of density functional theory and magnetic dipole-dipole energy calculations as well as a perturbation theory treatment of the spin-orbit coupling. We find that the spin orientation observed for these spin-1/2 ions is not caused by their anisotropic spin exchange interactions, nor by their magnetic dipole-dipole interactions, but by the spin-orbit coupling associated with their crystal-field split d-states. Our study also predicts in-plane anisotropy for the Cu^{2+} ions of Bi_2CuO_4 and Li_2CuO_2 . The results of our investigations dispel the mistaken belief that magnetic systems with spin-1/2 ions have no magnetic anisotropy induced by spin-orbit coupling.

I. Introduction

It is commonly believed that magnetic systems made up of spin-1/2 transition-metal ions have no magnetic anisotropy arising from spin-orbit coupling (SOC).¹ Thus the preferred spin orientation observed for such systems has been accounted for by invoking anisotropic spin exchange (ASE) or magnetic dipole-dipole (MDD) interactions between the spin-1/2 ions, as carried out, for example, by Moriya and Yoshida in their study of the Cu^{2+} ($S = 1/2$) spin orientation in $\text{CuCl}_2 \cdot 2\text{H}_2\text{O}$ six decades ago.^{1a} This conventional belief arises from the effective spin approximation,² in which magnetic ions are treated as spin-only ions and the effect of their unquenched orbital moments is included into anisotropic g-factors.^{2,3} For a magnetic ion such as

Cu^{2+} with nondegenerate magnetic orbital, the effective spin approximation reduces the SOC Hamiltonian $\hat{H}_{\text{SO}} = \lambda \hat{\mathbf{S}} \cdot \hat{\mathbf{L}}$ to the zero-field Hamiltonian,

$$\hat{H}_{\text{zf}} = D \left(\hat{S}_z^2 - \frac{1}{3} \hat{S}^2 \right) + \frac{1}{2} E \left(\hat{S}_+ \hat{S}_+ + \hat{S}_- \hat{S}_- \right), \quad (1)$$

where the constants D and E are related to the unquenched orbital angular momenta along the three local x-, y- and z-directions of the ion, which may be denoted as $\delta L_{\parallel x}$, $\delta L_{\parallel y}$ and $\delta L_{\parallel z}$, respectively, although they are not quantities to calculate or measure directly. If we take the local z-axis along the “axial” direction of a magnetic ion (located at a certain coordinate site), then the local x- and y-axes lie in the “equatorial” plane. In terms of the unquenched orbital momenta, the constant D is expressed as $D \propto \lambda^2 (\delta L_{\parallel z} - \delta L_{\perp z})$, where $\delta L_{\perp z} = (\delta L_{\parallel x} + \delta L_{\parallel y}) / 2$, and describes the difference between the “axial” and “equatorial-plane” components.³ The constant E, written as $E \propto \lambda^2 (\delta L_{\parallel x} - \delta L_{\parallel y})$, describes the anisotropy within the equatorial plane.³ The three states of an S=1 ion, $|1, -1\rangle$, $|1, 0\rangle$ and $|1, +1\rangle$, are split by \hat{H}_{zf} hence explaining the magnetic anisotropy of such a magnetic ion in the absence of an external magnetic field. In contrast, the two states of an S=1/2 ion, $|\uparrow\rangle = \left| \frac{1}{2}, +\frac{1}{2} \right\rangle$ and $|\downarrow\rangle = \left| \frac{1}{2}, -\frac{1}{2} \right\rangle$, are not split by \hat{H}_{zf} because $\langle \uparrow | \hat{H}_{\text{zf}} | \downarrow \rangle = 0$, as required by the Kramers degeneracy theorem for odd-spin ions.⁴

Thus, as far as the zero-field Hamiltonian is concerned, any S=1/2 ion cannot have magnetic anisotropy induced by SOC. So far, however, it has not been questioned whether this conclusion arising solely from the model Hamiltonian \hat{H}_{zf} is relevant at all for describing real magnetic compounds (e.g., molecules and solids) possessing S=1/2 ions, which are experimentally found to exhibit magnetic anisotropy. That the effective spin approximation cannot describe the magnetocrystalline anisotropy of systems with S=1/2 ions has been pointed out earlier in the study⁵ of $\text{Y}_2\text{V}_2\text{O}_7$ containing V^{4+} (d^1 , $S = 1/2$) ions at slightly-distorted

octahedral sites. Surprisingly, there has been no systematic study concerning whether or not magnetic compounds with $S=1/2$ ions have SOC-driven magnetic anisotropy.

In this work we probe this question by examining the cause for the observed spin orientations of the Cu^{2+} ($S = 1/2$) ions in $\text{CuCl}_2 \cdot 2\text{H}_2\text{O}$, LiCuVO_4 , CuCl_2 , CuBr_2 , Bi_2CuO_4 and Li_2CuO_2 , in which the Cu^{2+} ions are located at CuL_4 ($L = \text{O}, \text{Cl}, \text{Br}$) square-planar sites. On the basis of density functional theory (DFT) calculations, MDD energy calculations, and a perturbation theory analysis using \hat{H}_{SO} as perturbation, we show that the preferred orientation of the Cu^{2+} spins in these compounds is not caused by their ASE interactions, nor by their MDD interactions. It is caused by their single-ion anisotropy (SIA), namely, their SOC-driven magnetic anisotropy, which results when the crystal-field-split d-states of each magnetic ion Cu^{2+} interact under the action of SOC.

II. Computational Details

Our spin-polarized DFT calculations employed the projector augmented wave method encoded in the Vienna ab initio simulation package (VASP) ⁶ and the generalized gradient approximation of Perdew, Burke and Ernzerhof ⁷ for the exchange-correlation functionals with the plane wave cutoff energies of 400 eV, and the threshold of self-consistent-field (SCF) energy convergence of 10^{-6} eV. To describe the electron correlation associated with the Cu 3d states, we employed the DFT plus on-site repulsion U (DFT+U) method of Liechtenstein et al. ⁸ with an effective $U_{\text{eff}} = U - J = 4, 5$ and 6 eV on the Cu atom and the exchange-correction $J = 1$ eV since our calculations include noncollinear magnetic structures as well. ⁹ Preferred spin orientations were examined by performing DFT+U calculations including SOC (DFT+U+SOC) with the threshold of SCF energy convergence of 10^{-8} eV, and also by MDD energy calculations. ¹⁰ In

summing the MDD interactions between various pairs of spin sites, we employed the Ewald summation method.¹¹ In the VASP code the effect of SOC is treated by the second-variation method.¹² The DFT+U+SOC approach the present work employs has been successfully used to explain the magnetic anisotropy of, for example, SrFeO₂¹³ and TbMnO₃.¹⁴

III. Results and Discussion

Before we present our results in the following, it is worthwhile to briefly mention the various terms of a spin Hamiltonian employed to describe the magnetic properties of a material with localized electrons. When there is no SOC, the spin Hamiltonian is expressed as

$$\hat{H}_{\text{spin}} = -\sum_{i<j} J_{ij} \hat{\mathbf{S}}_i \cdot \hat{\mathbf{S}}_j = \sum_{i<j} J_{ij} (\hat{S}_{ix} \hat{S}_{jx} + \hat{S}_{iy} \hat{S}_{jy} + \hat{S}_{iz} \hat{S}_{jz}) \quad (2a)$$

with the isotropic Heisenberg exchange interactions J_{ij} between spins at the sites i and j . In the presence of SOC, these interactions can become anisotropic, i.e., they may become different along the x -, y - and z -directions ($J_{ij-x} \neq J_{ij-y} \neq J_{ij-z}$). In such a case, Eq. (2a) should be rewritten as

$$\hat{H}_{\text{spin}} = -\sum_{i<j} (J_{ij-x} \hat{S}_{ix} \hat{S}_{jx} + J_{ij-y} \hat{S}_{iy} \hat{S}_{jy} + J_{ij-z} \hat{S}_{iz} \hat{S}_{jz}) \quad (2b)$$

With the sign convention chosen for the spin Hamiltonians in Eqs. (2a) and (2b), the spin exchange constants (i.e., J_{ij} , J_{ij-x} , J_{ij-y} , J_{ij-z}) are antiferromagnetic (AFM) if they are negative, but ferromagnetic (FM) if they are positive.

In the presence of SOC, a spin Hamiltonian can be generally expressed as¹⁵

$$\hat{H}_{\text{spin}} = -\sum_{i<j} (J_{ij-x} \hat{S}_{ix} \hat{S}_{jx} + J_{ij-y} \hat{S}_{iy} \hat{S}_{jy} + J_{ij-z} \hat{S}_{iz} \hat{S}_{jz}) + \sum_{i<j} \vec{D}_{ij} \cdot (\hat{\mathbf{S}}_i \times \hat{\mathbf{S}}_j) + \sum_i A_i S_{iz}^2 \quad (2c)$$

where the second term the anisotropic antisymmetric exchange (i.e., Dzyaloshinskii-Moriya) interactions between spins at the sites i and j . The third term represents the SOC-driven magnetic

anisotropy of the spin at each site i , which occurs when the crystal-field-split d-states of a Cu^{2+} ion at the site i interact through SOC, namely, the SIA of the Cu^{2+} ion at the site i . Here the local z-axis at each Cu^{2+} ion site is taken along the direction perpendicular to its equatorial plane of the axially-elongated CuL_6 ($L = \text{O}$, halogen) octahedron. It should be emphasized that the third term of Eq. (2c) employs the z-component S_z of the classical spin vector \vec{S}_i instead of the quantum mechanical operator \hat{S}_{iz} . Each SIA term $A_i S_{iz}^2$ shows that the spin \vec{S}_i will orient along the local z-axis (easy-axis anisotropy) if $A_i < 0$, but perpendicular to the local z-axis (easy-plane anisotropy) if $A_i > 0$. (A more general expression for SIA is discussed in the Supplementary Material.¹⁶ For our discussion of the easy-axis vs. easy-plane anisotropy, the simplified expression given by the third term of Eq. (2c) is sufficient.) For various practical calculations, the spin operators \hat{S}_i and \hat{S}_j in the first and second terms of Eq. (2c) are treated as the classical spin vectors \vec{S}_i and \vec{S}_j , respectively.

A. $\text{CuCl}_2 \cdot 2\text{H}_2\text{O}$

In the crystal structure of $\text{CuCl}_2 \cdot 2\text{H}_2\text{O}$, isolated $\text{CuCl}_2(\text{OH}_2)_2$ complexes form skewed stacks along the b-direction (**Fig. 1a**) (in the setting of the standard space group Pmna),¹⁷ and in each $\text{CuCl}_2(\text{OH}_2)_2$ complex the linear O-Cu-O unit is perpendicular to the linear Cl-Cu-Cl unit. The $\text{CuCl}_2(\text{OH}_2)_2$ complexes form skewed-stack chains along the b-direction (**Fig. 1b**), and there are two chains per unit cell. The spin at each Cu^{2+} site is oriented along the Cu-O bond (i.e., lies in the CuCl_2O_2 plane), and the Cu^{2+} spins have an AFM coupling within each skewed stack but a FM coupling between adjacent stacks (**Fig. 1c**).¹⁸ We examine the cause for this easy-plane anisotropy as described below.

(1) We design an “isolated Cu^{2+} ion” model (Model I) by substituting Mg^{2+} ions for Cu^{2+} ions such that a (2a, 3b, 2c) supercell containing one Cu^{2+} ion repeats. The local coordinate axes

of an isolated $\text{CuCl}_2(\text{OH}_2)_2$ complex were chosen as depicted in **Fig. 1d**, where the local x- and y-axes are taken along the Cu-Cl and Cu-O bonds, respectively. Our DFT+U+SOC calculations for the “isolated Cu^{2+} ion” model with the spin orientations taken along the Cu-O bonds (i.e., $\parallel xy$) and perpendicular to the CuCl_2O_2 plane (i.e., $\perp xy$) show that the $\parallel xy$ orientation is more stable than the $\perp xy$ orientation (**Table I**). Because both the spin exchange and MDD interactions between adjacent Cu^{2+} ions are negligible in this “isolated Cu^{2+} ion” model, this result shows that the easy-plane anisotropy is an intrinsic property of an isolated $\text{CuCl}_2(\text{OH}_2)_2$ complex.

(2) We construct an “isolated Cu^{2+} chain model” in which, of two chains per unit cell, all Cu^{2+} ions in one chain are replaced with nonmagnetic Mg^{2+} ions, and examine the $\uparrow\downarrow\uparrow\downarrow$ and $\uparrow\uparrow\downarrow\downarrow$ spin arrangements along the “isolated Cu^{2+} chain” (to be referred to as Models II and III, respectively). For each of these two spin arrangements, we carry out DFT+U+SOC calculations for the $\parallel xy$ and $\perp xy$ spin orientations. (In the $\parallel xy$ spin orientation, the spin is aligned along the Cu-O bond, as found experimentally. See below for further discussion.) As for the spin exchange of the “isolated Cu^{2+} chain”, we consider only the nearest-neighbor exchange J_{nn} along the chain since the next-nearest-neighbor exchange J_{nnn} is negligible owing to the very long Cu...Cu distance (7.482 Å) involved. Given the AFM spin order along the stacking direction, it is reasonable to assume that the components J_{nn-x} , J_{nn-y} and J_{nn-z} of the nearest-neighbor exchange are all AFM. Given the convention that a negative spin exchange constant represents an AFM interaction, the spin exchange interaction energy per spin site for the $\uparrow\downarrow\uparrow\downarrow$ arrangement is given by

$$-J_{nn-x}S_{1x}S_{2x} - J_{nn-y}S_{1y}S_{2y} - J_{nn-z}S_{1z}S_{2z}, \quad (3)$$

where two adjacent spin sites are labeled as 1 and 2 for convenience. Then, the $\parallel xy$ spin orientation is explained if $|J_{nn-x}|, |J_{nn-y}| > |J_{nn-z}|$. In the $\uparrow\uparrow\downarrow\downarrow$ arrangement the sum of the nearest-neighbor spin exchange interaction energies is zero, so the $\parallel xy$ and $\perp xy$ spin orientations would

be identical in energy if the ASE interactions were the cause for the spin orientation. However, **Table I** shows that the preference for the in-plane spin orientation is practically identical in both $\uparrow\downarrow\uparrow\downarrow$ and $\uparrow\uparrow\downarrow\downarrow$ arrangements. This reveals that the ASE interactions are not responsible for the easy-plane anisotropy of the Cu^{2+} ion.

We use the “isolated Cu^{2+} chain” model to evaluate the values of J_{nn-x} , J_{nn-y} and J_{nn-z} by using the energy-mapping analysis.¹⁵ To obtain J_{nn-x} , we consider the FM and AFM spin arrangements with spins collinear to the x-direction. Representing the energies of these two state by $E(\uparrow\uparrow)_x$ and $E(\uparrow\downarrow)_x$, respectively, we obtain

$$J_{nn-x} = [E(\uparrow\uparrow)_x - E(\uparrow\downarrow)_x]/2. \quad (4a)$$

Thus J_{nn-x} is determined by obtaining the energy difference, $E(\uparrow\uparrow)_x - E(\uparrow\downarrow)_x$, on the basis of DFT+U+SOC calculations. The values of J_{nn-y} and J_{nn-z} are similarly determined.

$$J_{nn-y} = [E(\uparrow\uparrow)_y - E(\uparrow\downarrow)_y]/2 \quad (4b)$$

$$J_{nn-z} = [E(\uparrow\uparrow)_z - E(\uparrow\downarrow)_z]/2 \quad (4c)$$

Our results summarized in **Table II** show that there is practically no anisotropy in the spin exchange constants. This also reveals that the easy-plane anisotropy of the Cu^{2+} ion is not caused by the ASE interactions.

(3) We examine the MDD energies for two spin configurations, namely, the $\uparrow\downarrow\uparrow\downarrow$ and $\uparrow\uparrow\downarrow\downarrow$ arrangements within each skewed stack of Cu^{2+} ions but with FM spin arrangement between adjacent stacks. For each of these spin arrangements, we calculate the MDD energies with the \parallel_{xy} and \perp_{xy} spin orientations to find that the energy difference, $E_{\parallel xy} - E_{\perp xy}$, between the two spin orientations is negligibly small (i.e., +0.005 and -0.014 meV/Cu for the $\uparrow\downarrow\uparrow\downarrow$ and $\uparrow\uparrow\downarrow\downarrow$ arrangements, respectively). This clearly shows that MDD interactions cannot be responsible for the easy-plane anisotropy of the Cu^{2+} spin in $\text{CuCl}_2 \cdot 2\text{H}_2\text{O}$.

(4) The above discussion shows beyond any doubt that the easy-plane anisotropy of the Cu^{2+} spin in $\text{CuCl}_2 \cdot 2\text{H}_2\text{O}$ is an intrinsic property of an isolated $\text{CuCl}_2(\text{OH}_2)_2$ complex that is associated with SOC. The two spin directions of interest in the $\parallel xy$ spin orientation are the Cu-O and Cu-Cl bond directions. Our DFT+U+SOC calculations for the “isolated Cu^{2+} chain model” with FM spin arrangement reveal that the spin orientation along the Cu-O bond is more stable than that along the Cu-Cl bond by 0.10, 0.08 and 0.07 meV/Cu for effective $U_{\text{eff}} = 4, 5$ and 6 eV, respectively. The preference for the spin to orient along the Cu-O bond is in agreement with experiment.¹⁸

(5) Let us now demonstrate that the observed and calculated spin orientation of $\text{CuCl}_2(\text{OH}_2)_2$ is caused solely by SIA. By using the coordinate systems (x, y, z) and (x', y', z') for the orbital and spin, respectively, the SOC Hamiltonian $\hat{H}_{\text{SO}} = \lambda \hat{\mathbf{S}} \cdot \hat{\mathbf{L}}$ is expressed as^{3,15,19}

$$\begin{aligned} \hat{H}_{\text{SO}} = & \lambda \hat{S}_{z'} \left(\hat{L}_z \cos \theta + \frac{1}{2} \hat{L}_+ e^{-i\varphi} \sin \theta + \frac{1}{2} \hat{L}_- e^{i\varphi} \sin \theta \right) \\ & + \frac{\lambda}{2} \hat{S}_+ \left(-\hat{L}_z \sin \theta - \hat{L}_+ e^{-i\varphi} \sin^2 \frac{\theta}{2} + \hat{L}_- e^{i\varphi} \cos^2 \frac{\theta}{2} \right) \\ & + \frac{\lambda}{2} \hat{S}_- \left(-\hat{L}_z \sin \theta + \hat{L}_+ e^{-i\varphi} \cos^2 \frac{\theta}{2} - \hat{L}_- e^{i\varphi} \sin^2 \frac{\theta}{2} \right) \end{aligned} \quad (5)$$

Thus \hat{H}_{SO} is rewritten as $\hat{H}_{\text{SO}} = \hat{H}_{\text{SO}}^0 + \hat{H}'_{\text{SO}}$, where \hat{H}_{SO}^0 is the spin-conserving term (i.e., the first line of Eq. 1), and \hat{H}'_{SO} is the spin-non-conserving term (i.e., the second and third lines of Eq. 1). Then the preferred spin orientation (i.e., the z' axis) is along the z -axis (i.e., $\theta = 0^\circ$) for the easy-axis anisotropy, but perpendicular to the z -axis (i.e., $\theta = 90^\circ$) for the easy-plane anisotropy. It was shown earlier that the easy-plane anisotropy of the high-spin Fe^{2+} (d^6 , $S = 2$) ions in SrFeO_2 ¹³ and $\text{Sr}_3\text{Fe}_2\text{O}_5$ ¹⁰ as well as the easy-axis anisotropy of the high-spin Mn^{3+} (d^4 , $S = 2$) ions in TbMnO_3 ¹⁴ and Ag_2MnO_2 ²⁰ are well explained on the basis of a perturbation theory analysis by

using $\hat{H}_{\text{so}} = \lambda \hat{S} \cdot \hat{L}$ as perturbation and the crystal-field split d-states of a magnetic ion as unperturbed states.

When an occupied down-spin d-level $i = \psi_o \downarrow$ with energy e_i interacts with an unoccupied down-spin d-level $j = \psi_u \downarrow$ with energy e_j via the matrix element $\langle i | \hat{H}_{\text{so}}^0 | j \rangle$, the associated energy lowering is given by

$$\Delta E_{\text{soc}} = - \frac{|\langle i | \hat{H}_{\text{so}}^0 | j \rangle|^2}{|e_i - e_j|}. \quad (6)$$

In the following discussion we recall that, in terms of spherical harmonics Y_ℓ^m , the angular behavior of the d-orbitals are given by $z^2 \propto Y_2^0$, $xz \propto Y_2^1 - Y_2^{-1}$, $yz \propto Y_2^1 + Y_2^{-1}$, $xy \propto Y_2^2 - Y_2^{-2}$, and $x^2 - y^2 \propto Y_2^2 + Y_2^{-2}$. In determining the preferred spin orientation, the most important interaction is the one with the smallest energy gap ($e_i - e_j$). According to the split Cu 3d states of $\text{CuCl}_2 \cdot 2\text{H}_2\text{O}$ (**Fig. 1d**), the empty $(x^2 - y^2) \downarrow$ has the smallest energy gap with the filled $xz \downarrow$ state. (It should be pointed out that the split Cu 3d states determined from the DFT+U calculations do not violate Kramers degeneracy theorem. It is only by convention that the up-spin states are chosen as the majority-spin states, and the down-spin states as the minority-spin states. The alternative choice in which the down-spin states are chosen as the majority-spin states is equally valid, thereby maintaining the doublet degeneracy of a spin-1/2 system.) The magnetic orbital quantum number m of xz differs from that of $x^2 - y^2$ by 1 so that the matrix element $\langle xz \downarrow | \hat{H}_{\text{so}}^0 | (x^2 - y^2) \downarrow \rangle$ can be nonzero via the \hat{L}_+ and \hat{L}_- terms of \hat{H}_{so}^0 . Since these terms have the coefficient $\sin\theta$, the interaction between the $(x^2 - y^2) \downarrow$ and $xz \downarrow$ states predicts easy-plane anisotropy (i.e., $\theta = 90^\circ$). This matrix element also predicts the spin orientation along the Cu-O bond; given $\theta = 90^\circ$, the $\langle xz \downarrow | \hat{H}_{\text{so}}^0 | (x^2 - y^2) \downarrow \rangle$ term is rewritten as

$$\langle xz \downarrow | \hat{H}_{\text{SO}}^0 | (x^2 - y^2) \downarrow \rangle \propto \langle xz | \hat{L}_x \cos \phi + \hat{L}_y \sin \phi | x^2 - y^2 \rangle \propto \sin \phi, \quad (7)$$

because $\langle xz | \hat{L}_x | x^2 - y^2 \rangle = 0$ and $\langle xz | \hat{L}_y | x^2 - y^2 \rangle = -i$.³ Consequently, the matrix element $\langle xz \downarrow | \hat{H}_{\text{SO}}^0 | (x^2 - y^2) \downarrow \rangle$ is maximized for $\phi = 90^\circ$, i.e., the preferred spin orientation in the local xy-plane is along the Cu-O bond (**Fig. 1d**). In short, the easy-plane anisotropy of the Cu^{2+} ions in $\text{CuCl}_2 \cdot 2\text{H}_2\text{O}$ is solely explained by the SOC associated with its crystal-field split d-states, and is hence caused by SIA.

B. CuCl_2 , CuBr_2 and LiCuVO_4

We now demonstrate that SIA is also the origin of the easy-plane anisotropy for the Cu^{2+} ions in CuCl_2 ,^{21,22} CuBr_2 ²³ and LiCuVO_4 ,²⁴ in which the square planar CuL_4 units ($\text{L} = \text{Cl}, \text{Br}, \text{O}$) share their opposite edges to form CuL_2 ribbon chains (**Fig. 2a-c**). Neutron powder and single crystal diffraction studies showed that these Cu^{2+} spins prefer to lie in the planes of the CuL_4 units (i.e., easy-plane anisotropy). Furthermore, the spins in each CuL_2 ribbon chain has an incommensurate spin-spiral arrangement (**Fig. 2d**) due to the spin frustration arising from the competition of the FM nearest-neighbor spin exchange J_{nn} and the AFM next-nearest-neighbor spin exchange J_{nnn} .^{15,22-24} In the spin-spiral arrangements neighboring moments make an angle of $\sim 90^\circ$. We examine the cause for this easy-plane anisotropy as described below.

(1) To determine if this anisotropy is caused by the ASE interactions, we consider three different models of spin arrangements in each CuL_2 ribbon chain:

- a) One is the “isolated Cu^{2+} ion” model in which, of two ribbon chains per unit cell, all Cu^{2+} ions of one chain are replaced with Mg^{2+} ions while the other chain is converted to a $(\text{Cu}^{2+} - \text{Mg}^{2+} - \text{Mg}^{2+} - \text{Mg}^{2+})_\infty$ chain (**Fig. 2e**).

b) The second model has the $\uparrow\downarrow\uparrow\downarrow$ collinear arrangement of Cu^{2+} spins in each ribbon chain (**Fig. 2f**).

c) The third model has the $\uparrow\rightarrow\downarrow\leftarrow$ spin-spiral arrangement of Cu^{2+} spins in each ribbon chain (**Fig. 2d**).

For each of these spin arrangements, we carry out DFT+U+SOC calculations for the \parallel_{xy} and \perp_{xy} spin orientations to determine their relative energies. In the case of the spin-spiral arrangement (**Fig. 2d**), the \perp_{xy} spin orientation means that the plane of the spin spiral is perpendicular to the ribbon plane. In the \perp_{xy} spin spiral, therefore, each spin direction is $\pm 45^\circ$ away from the local $\pm z$ -axis. Our calculations for the “isolated Cu^{2+} ion” model show that the \parallel_{xy} orientation is more stable than the \perp_{xy} orientation (**Table III**), indicating that the easy-plane anisotropy is an intrinsic property of an isolated CuL_4 unit. The relative energies, $E_{\parallel_{xy}} - E_{\perp_{xy}}$, obtained from the $\uparrow\downarrow\uparrow\downarrow$ chain model are practically identical to those obtained from the “isolated Cu^{2+} ion” model, so the spin exchanges J_{nn} and J_{nnn} are not responsible for the easy-plane anisotropy. It is reasonable to assume that the components J_{nn-x} , J_{nn-y} and J_{nn-z} are all FM because J_{nn} is FM, while the components J_{nnn-x} , J_{nnn-y} and J_{nnn-z} are all AFM because J_{nnn} is AFM. Then, the preference for the \parallel_{xy} spin orientation is explained if $J_{nn-x}, J_{nn-y} > J_{nn-z}$ and/or if $|J_{nnn-x}|, |J_{nnn-y}| > |J_{nnn-z}|$. The $\uparrow\downarrow\uparrow\downarrow$ spin arrangement does not fulfil these conditions, but it shows the preference for the \parallel_{xy} spin orientation, just as the “isolated Cu^{2+} ion” model predicts. In the case of the spin-spiral arrangement as well, the \parallel_{xy} spin orientation is favored over the \perp_{xy} spin orientation (**Table III**). However, the energy difference, $E_{\parallel_{xy}} - E_{\perp_{xy}}$, for the spin-spiral arrangement is approximately half of that found for the $\uparrow\downarrow\uparrow\downarrow$ collinear spin arrangement. This is so because, for each spin of the out-of-plane spin spiral arrangement, only 50% has the \parallel_z spin

component. In short, the ASE interactions are not responsible for the observed easy-plane anisotropy.

(2) Our MDD energy calculations using the $\uparrow\downarrow\uparrow\downarrow$ spin arrangement in each CuL_2 ribbon chain show that the \perp_{xy} spin orientation is more stable than the \parallel_{xy} spin orientation by 0.07, 0.07 and 0.01 meV/Cu for LiCuVO_4 , CuCl_2 and CuBr_2 , respectively. However, these MDD interactions are too weak to influence the spin orientation.

(3) We now examine the crystal-field split Cu 3d states of CuCl_2 , CuBr_2 and LiCuVO_4 as well as their interaction under SOC. As a representative example, **Fig. 2g** shows the PDOS plots calculated for CuCl_2 (For the PDOS plots of LiCuVO_4 and CuBr_2 , see **Fig. S1** and **S2** of the Supplementary Material²⁵). We note that $\langle x^2 - y^2 | \hat{L}_\mu | x^2 - y^2 \rangle = 0$ for $\mu = x, y$ and z ,³ and $\langle z^2 \downarrow | \hat{H}_{\text{so}} | (x^2 - y^2) \downarrow \rangle = 0$ because the magnetic quantum number m of z^2 differs from those of $x^2 - y^2$ by 2. Consequently, **Fig. 2g** shows that the preferred spin orientation is determined by the interaction terms $\langle xy \downarrow | \hat{H}_{\text{so}} | (x^2 - y^2) \downarrow \rangle$ and $\langle (xz/yz) \downarrow | \hat{H}_{\text{so}} | (x^2 - y^2) \downarrow \rangle$. The filled $(xz/yz) \downarrow$ states are closer to the empty $(x^2 - y^2) \downarrow$ states than are the filled $xy \downarrow$ states so that the \parallel_{xy} spin orientation is favored over the \perp_{xy} spin orientation, in agreement with experiment. The in-plane anisotropy observed for CuBr_2 and LiCuVO_4 is similarly explained. Thus, just as found for $\text{CuCl}_2 \cdot 2\text{H}_2\text{O}$, the easy-plane anisotropy of the $S=1/2$ ions Cu^{2+} in CuCl_2 , CuBr_2 and LiCuVO_4 is caused by their SIA.

C. Bi_2CuO_4 and Li_2CuO_2

Bi_2CuO_4 consists of CuO_4 square planes stacked to form CuO_4 chains along the c -direction (**Fig. 3a**). Adjacent CuO_4 units in each chain are staggered, and adjacent CuO_4 chains are interlinked by Bi^{3+} ions, which form BiO_4 sawhorse units (not shown for simplicity). As summarized in **Table IV**, our DFT+U+SOC calculations show easy-plane anisotropy. Easy-axis anisotropy was reported for Bi_2CuO_4 in some experiments,^{26,27} but easy-plane anisotropy was concluded from other experiments.²⁸ These conflicting findings may be related to the quality of the Bi_2CuO_4 samples employed as can be seen from their bulk magnetic properties; the Curie-Weiss temperature of Bi_2CuO_4 is approximately -40 K in the studies reporting easy-axis anisotropy,²⁶ but was found close to -100 K in the studies reporting easy-plane anisotropy.²⁸ Furthermore, the neutron diffraction study concluding easy-axis anisotropy employed a powder sample,²⁶ but that concluding easy-plane anisotropy a single crystal sample.^{28a} The magnetic diffraction intensities are more sensitive to the moment direction for a single crystal than for a powder sample.

Li_2CuO_2 consists of CuO_2 ribbon chains of edge-sharing CuO_4 square planes (**Fig. 3b**), and the neutron diffraction studies²⁹ show that the Cu^{2+} spins in each ribbon chain have a FM coupling, essentially with easy-axis anisotropy (the reported spin orientation is slightly tilted away from the local z -axis of each CuO_4 square plane, i.e., from the crystallographic c -direction, in ref. 29b). The absence of a spin spiral order and the adoption of an FM order in the CuO_2 ribbon chains of Li_2CuO_2 have been explained as a consequence of order by disorder induced by next-nearest-neighbor interchain spin exchange interactions.³⁰ Just as found for all other $S=1/2$ systems discussed above, our DFT+U+SOC calculations predict easy-plane anisotropy for Li_2CuO_2 (**Table V**), in apparent contradiction to the experimental finding.²⁹ However, it should be pointed out that the order-by-disorder state is not properly simulated by a few ordered spin

states employed in our DFT+U+SOC calculations. Further studies are necessary to resolve this discrepancy.

IV. Concluding remarks

In summary, the observed easy-plane anisotropy of the $S=1/2$ Cu^{2+} ions in $\text{CuCl}_2 \cdot 2\text{H}_2\text{O}$, LiCuVO_4 , CuCl_2 and CuBr_2 is not caused by their ASE interactions, nor by their MDD interactions. Our study clearly reveals that its origin is the SIA, namely, the SOC-driven magnetic anisotropy, which results when the crystal-field-split d-states of each magnetic ion Cu^{2+} interact under the action of SOC. An $S=1/2$ ion should possess SIA unless the magnetic orbital accommodating an unpaired electron is triply degenerate as found in $\text{Ba}_2\text{NaOsO}_6$,³¹ so most $S=1/2$ ions should exhibit SIA. It is necessary to dispel the mistaken belief that magnetic systems with spin-1/2 ions have no SOC-induced magnetic anisotropy. In superconducting precursor La_2CuO_4 , calculations show the Cu^{2+} ions to possess easy-plane anisotropy,⁵ and the presence of SIA at each Cu^{2+} site is not prevented by any symmetry consideration. Thus, it would be interesting to see if the SIA of Cu^{2+} ions affects the spin fluctuation in cuprates³² believed to be the key to understanding their superconductivity.

Acknowledgments

This research was supported by the computing resources of the NERSC center and the HPC center of NCSU. Work at Fudan was partially supported by NSFC, FANEDD, NCET-10-0351, Research Program of Shanghai Municipality and MOE, the Special Funds for Major State Basic Research, Program for Professor of Special Appointment (Eastern Scholar), and Fok Ying Tung Education Foundation.

e-mails: hxiang@fudan.edu.cn, mike_whangbo@ncsu.edu

References

1. (a) T. Moriya and K. Yoshida, Prog. Theoret. Phys. **9**, 663 (1953). (b) For example, see the lecture note of M. Suzuki and I. Suzuki on spin Hamiltonian of transition metal ions in crystal field, <http://www2.binghamton.edu/physics/docs/crystal-field6-15-07.pdf>.
2. (a) M. H. L. Pryce, Proc. Phys. Soc. A **63**, 25 (1950). (b) N. Majlis, The Quantum Theory of Magnetism (World Scientific, Singapore, 2000).
3. D. Dai, H. J. Xiang and M.-H. Whangbo, J. Comput. Chem. **29**, 2187 (2008).
4. H. A. Kramers, Proc. Amsterdam Acad. **33**, 959 (1930).
5. H. J. Xiang, E. J. Kan, M.-H. Whangbo, C. Lee, S.-H. Wei and X. G. Gong, Phys. Rev. B **83**, 174402 (2011).
6. (a) G. Kresse and J. Hanfner, Phys. Rev. B **47**, 558 (1993). (b) G. Kresse and J. Furthmüller, Comput. Mater. Sci. **6**, 15 (1996). (c) G. Kresse and J. Furthmüller, Phys. Rev. B. **54**, 11169 (1996).
7. J. P. Perdew, S. Burke and M. Ernzerhof, Phys. Rev. Lett. **77**, 3865 (1996).
8. A. I. Liechtenstein, V. I. Anisimov and J. Zaanen, Phys. Rev. B **52**, 5467 (1995).
9. E. Bousquet and N. Spaldin, Phys. Rev. B **82**, 220402 (2010).
10. H.-J. Koo, H. J. Xiang, C. Lee and M.-H. Whangbo, Inorg. Chem. **48**, 9051 (2009).
11. (a) P. P. Ewald, Ann. Phys. **64**, 253 (1921). (b) T. Darden, D. York and L. Pedersen, J. Chem. Phys. **98**, 10089 (1993). (c) H. Wang, F. Dommert and C. Holm, J. Chem. Phys. **133**, 034117 (2010).
12. D. D. Koelling and B. N. Harmon, J. Phys. C **10**, 3107 (1977).

13. H. J. Xiang, S.-H. Wei, and M.-H. Whangbo, Phys. Rev. Lett. **100**, 167207 (2008).
14. H. J. Xiang, S.-H. Wei, M.-H. Whangbo, and J. L. F. Da Silva, Phys. Rev. Lett. **101**, 037209 (2008).
15. H. J. Xiang, C. Lee, H.-J. Koo, X. G. Gong and M.-H. Whangbo, Dalton Trans. **42**, 823 (2013).
16. See Supplementary Material Document No. _____ for the general expression of single ion anisotropy. For information on Supplementary Material, see <http://www.aip.org/pubservs/epaps.html>.
17. S. Brownstein, N. F. Han, E. J. Gabe, and Y. le Page, Y. Zeitschrift Kristallogr. **189**, 13 (1989).
18. N. J. Poulis and G. E. G. Haderman, Physica 18, 201 (1952).
19. X. Wang, R. Wu, D.-S. Wang and A. J. Freeman, Phys. Rev. B **54**, 61 (1996).
20. S. Ji, E. J. Kan, M.-H. Whangbo, J.-H. Kim, Y. Qiu, M. Matsuda, H. Yoshida, Z. Hiroi, M. A. Green, T. Ziman, and S.-H. Lee, Phys. Rev. B **81**, 094421 (2010).
21. M. G. Banks, R. K. Kremer, C. Hoch, A. Simon, B. Ouladdiaf, J.-M. Broto, H. Rakoto, C. Lee and M.-H. Whangbo, Phys. Rev. B **80**, 024404 (2009).
22. L. Zhao, T.-L. Hung, C.-C. Li, Y.-Y. Chen, M.-K. Wu, R. K. Kremer, M. G. Banks, A. Simon, M.-H. Whangbo, C. Lee, J. S. Kim, I. G. Kim and K. H. Kim, Adv. Mater. **24**, 2469 (2012).
23. (a) D. Dai, H.-J. Koo and M.-H. Whangbo, Inorg. Chem. **43**, 4026 (2004). (b) H.-J. Koo, C. Lee, M.-H. Whangbo, G. J. McIntyre and R. K. Kremer, Inorg. Chem. **50**, 3582 (2011).
24. B. J. Gibson, R. K. Kremer, A. V. Prokofiev, W. Assmus and G. J. McIntyre, Physica B **350**, e253 (2004).

25. See Supplementary Material Document No. _____ for the PDOS plots calculated for LiCuVO_4 and CuBr_2 . For information on Supplementary Material, see <http://www.aip.org/pubservs/epaps.html>.
26. J. P. Attfield, *J. Phys.: Condens. Matter.* **1**, 7045 (1989).
27. (a) J. L. Garcia-Munoz, J. Roderiguez-Carvajal, F. Sapina, M. J. Sanchis, R. Ibanez and D. Beltran-Porter, *J. Phys. Condens. Matter.* **2**, 2205 (1990). (b) B. D. White, W. M. Pätzold and J. J. Neumeier, *Phys. Rev. B.* **82**, 094439 (2010).
28. (a) K. Yamada, K.-I. Takada, S. Hosoya, Y. Watanabe, Y. Endoh, N. Tomonaga, T. Suzuki, T. Ishigaki, T. Kamiyama, H. Asano and F. Izumi, *J. Phys. Soc. Jpn.* **60**, 2406 (1991). (b) M. Herak, M. Miljak, G. Dhalenne and A. Revcolevschi, *J. Phys.: Condens. Matter.* **22**, 026006 (2010).
29. (a) F. Sapina, J. Rodriguez Carvajal, M. J. Sanchis, R. Ibanez, A. Beltran and D. Beltran, *Solid State Commun.* **74**, 779 (1990). (b) E. M. L. Chung, G. J. McIntyre, D. McK. Paul, G. Balakrishnan, and M. R. Lees, *Phys. Rev. B* **68**, 144410 (2003).
30. H. J. Xiang, C. Lee and M.-H. Whangbo, *Phys. Rev. B: Rapid Commun.* **76**, 220411(R) (2007).
31. H. J. Xiang and M.-H. Whangbo, *Phys. Rev. B* **75**, 052407 (2007).
32. For example, see: E. Demler and S.-C. Zhang, *Nature* **396**, 733 (1998).

Table I. The energy (in meV/Cu) of the $\parallel xy$ spin orientation with respect to that of the $\perp xy$ spin orientation, $E_{\parallel xy} - E_{\perp xy}$, obtained from the DFT+U+SOC calculations for three models of $\text{CuCl}_2 \cdot 2\text{H}_2\text{O}$.^a

U_{eff}	4 eV	5 eV	6 eV
Model I ^b	-0.36	-0.32	-0.27
Model II ^c	-0.23	-0.20	-0.17
Model III ^d	-0.23	-0.20	-0.18

^a In the $\parallel xy$ spin orientation, the spin is parallel to the Cu-O bond.

^b “Isolated Cu^{2+} ion” model

^c “Isolated Cu^{2+} chain” model with $\uparrow\downarrow\uparrow\downarrow$ spin arrangement

^d “Isolated Cu^{2+} chain” model with $\uparrow\uparrow\downarrow\downarrow$ spin arrangement

Table II. The values of the three components $J_{\text{nn-x}}$, $J_{\text{nn-y}}$ and $J_{\text{nn-z}}$ (in meV) of the nearest-neighbor spin exchange J_{nn} in $\text{CuCl}_2 \cdot 2\text{H}_2\text{O}$ determined from DFT+U+SOC calculations.

	$U_{\text{eff}} = 4 \text{ eV}$	$U_{\text{eff}} = 5 \text{ eV}$	$U_{\text{eff}} = 6 \text{ eV}$
$J_{\text{nn-x}}$	-1.335	-1.090	-0.885
$J_{\text{nn-y}}$	-1.335	-1.090	-0.890
$J_{\text{nn-z}}$	-1.335	-1.095	-0.890

Table III. The relative energies, $E_{\parallel xy} - E_{\perp xy}$, in meV/Cu obtained from DFT+U+SOC calculations for the “isolated Cu^{2+} ion” model, the $\uparrow\downarrow\uparrow\downarrow$ chain model (in parenthesis), and the $\uparrow\rightarrow\downarrow\leftarrow$ spin-spiral chain model (in square bracket).

	$U_{\text{eff}} = 4 \text{ eV}$	$U_{\text{eff}} = 5 \text{ eV}$	$U_{\text{eff}} = 6 \text{ eV}$
LiCuVO_4	-0.35 ^a , (-0.36) ^b , [-0.18] ^c	-0.31 ^a , (-0.31) ^b , [-0.17] ^c	-0.26 ^a , (-0.27) ^b , [-0.14] ^c
CuCl_2	-0.29, (-0.26), [-0.15]	-0.23, (-0.22), [-0.13]	-0.21, (-0.19), [-0.12]
CuBr_2	-0.13, (-0.16), [-0.07]	-0.11, (-0.14), [-0.06]	-0.10, (-0.12), [-0.05]

^a The “isolated Cu^{2+} ion” model

^b The $\uparrow\downarrow\uparrow\downarrow$ chain model

^c The $\uparrow\rightarrow\downarrow\leftarrow$ spin-spiral chain model

Table IV. The relative energies in meV/Cu obtained for the three spin orientations of Bi₂CuO₄ from DFT+U+SOC calculations for the experimentally observed AFM state.^a

Spin orientation	U _{eff} = 4 eV	U _{eff} = 6 eV
//a	-0.56	-0.38
//b	-0.56	-0.38
//c	0	0

^a The Cu²⁺ spins in each CuO₄ chain are antiferromagnetically coupled, and so are those between adjacent CuO₄ chains such that, in **Fig. 3**, the Cu²⁺ ion of the upper CuO₄ unit in the left CuO₄ chain makes an AFM coupling with the corresponding one in the right CuO₄ chain.

Table V. The relative energies, E_{||xy} - E_{⊥xy}, in meV/Cu of Li₂CuO₂ obtained from DFT+U+SOC calculations for the “isolated Cu²⁺ ion”, the ↑↓↑↓ chain, and the ↑↑↓↓ chain models.

	U _{eff} = 4 eV	U _{eff} = 6 eV
“isolated Cu ²⁺ ion”	0.34	0.28
↑↓↑↓ chain	0.25	0.23
↑↑↓↓ chain	0.30	0.24

Figure captions

Figure 1. (Color online) (a) A perspective view of the crystal structure of $\text{CuCl}_2 \cdot 2\text{H}_2\text{O}$ (blue circle: Cu, yellow circle: Cl, red circle: O, white circle: H). (b) A schematic view of an isolated $\text{CuCl}_2(\text{OH}_2)_2$ chain along the b-direction. (c) The magnetic structure of $\text{CuCl}_2 \cdot 2\text{H}_2\text{O}$, where the filled and unfilled circles represent up-spin and down-spin Cu^{2+} sites, respectively. (d) The local coordinate system chosen for an isolated $\text{CuCl}_2(\text{OH}_2)_2$ complex with the crystal-field split Cu 3d states. (e) The PDOS plots calculated for the Cu 3d states of $\text{CuCl}_2 \cdot 2\text{H}_2\text{O}$ using the “isolated Cu^{2+} ion” model, where the horizontal axis refers to energy in eV (with the Fermi level $E_F = 0$), and the vertical axis the PDOS in states/eV/Cu (with the up-spin and down-spin states represented by positive and negative numbers, respectively).

Figure 2. (Color online) (a) Arrangement of CuL_2 ribbon chains (along the crystallographic b-direction) in CuL_2 ($L = \text{Cl}, \text{Br}$), where the Cu and L atoms are represented by blue and green spheres, respectively. (b) Arrangement of CuO_2 ribbon chains (along the crystallographic b-direction) in LiCuVO_4 , where the Cu and O atoms are represented by blue and red spheres, respectively. (c) A schematic view of a CuL_2 ($L = \text{Cl}, \text{Br}, \text{O}$) ribbon chain found in CuCl_2 , CuBr_2 and LiCuVO_4 . (d) A schematic view of the $\uparrow \rightarrow \downarrow \leftarrow$ spin-spiral arrangement in the CuL_2 ribbon chain, for the case when the spin-spiral plane is the xy-plane. (e) An “isolated Cu^{2+} ion” model, in which a chain of Cu^{2+} ions is replaced with a $(\text{Cu}^{2+} - \text{Mg}^{2+} - \text{Mg}^{2+} - \text{Mg}^{2+})_\infty$ chain. (f) A schematic view of the $\uparrow \downarrow \uparrow \downarrow$ collinear arrangement of Cu^{2+} spins in the CuL_2 ribbon chain, for the case when the spins lie in the xy-plane. (g) The PDOS plots calculated for the Cu 3d states of CuCl_2 , where the horizontal axis refers to energy in eV (with the Fermi level $E_F = 0$), and the vertical

axis the PDOS in states/eV/Cu (with the up-spin and down-spin states represented by positive and negative numbers, respectively).

Figure 3. (Color online) (a) Perspective view of the stacked CuO_4 square planes (along the crystallographic c-direction) in Bi_2CuO_4 . (b) Arrangement of the CuO_2 ribbon chains (along the crystallographic b-direction) in LiCuVO_4 . Here the Cu and O atoms are represented by blue and red spheres, respectively.

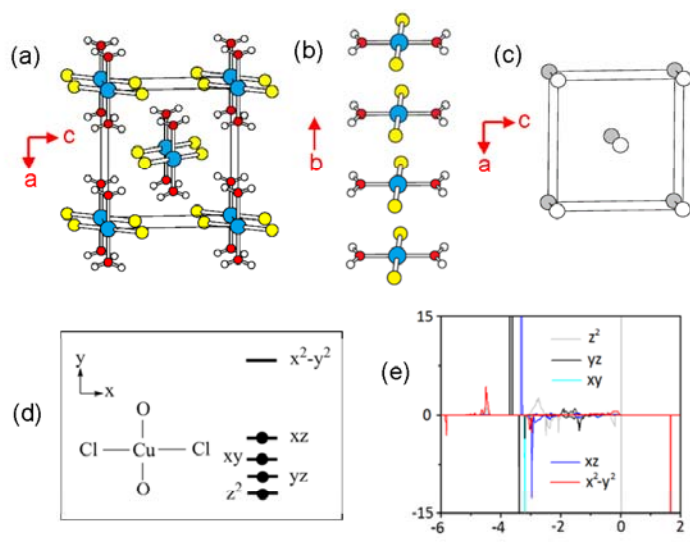


Fig. 1

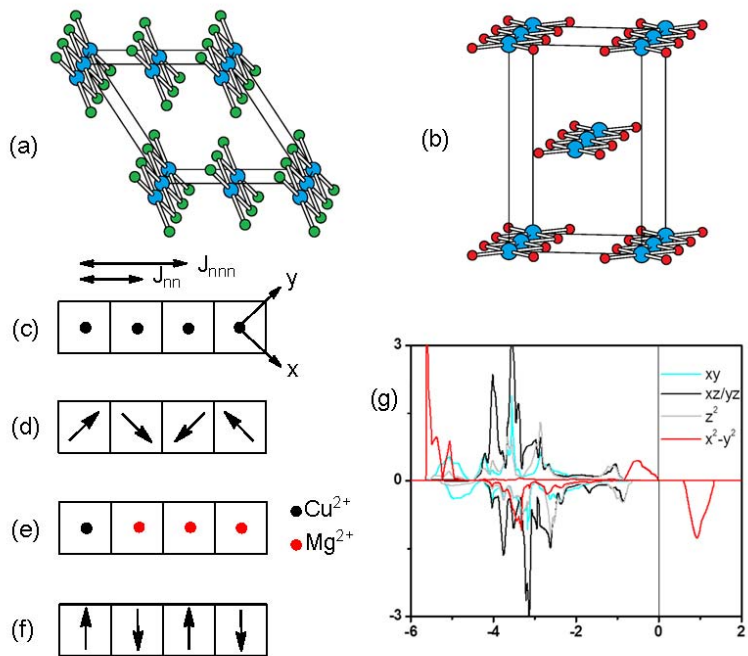


Fig. 2

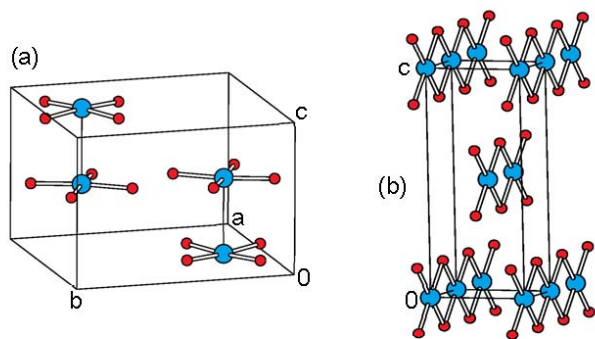


Fig. 3

Most spin-1/2 transition-metal ions do have single ion anisotropy

Jia Liu¹, Hyun-Joo Koo², Hongjun Xiang^{3,*}, Reinhard K. Kremer⁴ and Myung-Hwan Whangbo^{1,*}

¹ Department of Chemistry, North Carolina State University, Raleigh, North Carolina 27695, USA

² Department of Chemistry and Research Institute for Basic Sciences, Kyung Hee University, Seoul 130-701, Republic of Korea

³ Key Laboratory of Computational Physical Sciences (Ministry of Education), State Key Laboratory of Surface Physics, and Department of Physics, Fudan University, Shanghai 200433, People's Republic of China

⁴ Max-Planck-Institut für Festkörperforschung, Heisenbergstrasse 1, D-70569 Stuttgart, Germany

1. Single ion anisotropy

The SIA of a magnetic ion i is more generally discussed in terms of the term^{1,2}

$$\mathbf{S}_i \cdot \mathbf{D} \cdot \mathbf{S}_i, \quad (\text{S1})$$

where \mathbf{D} represents the second-order anisotropy tensor while \mathbf{S}_i is treated as the vector operator.

In the local coordinate system that diagonalizes \mathbf{D} to give the diagonal elements D_{xx} , D_{yy} and D_{zz} , Eq. (S1) can be replaced with^{2a,3}

$$AS_{iz}^2 + B(S_{ix}^2 - S_{iy}^2), \quad (\text{S2})$$

where $A = D_{zz} - (D_{xx} + D_{yy})/2$ and $B = (D_{xx} - D_{yy})/2$. In general, for Cu^{2+} (d^9 , $S=1/2$) ions that are typically found in axially-elongated octahedral coordinate sites, square pyramidal or square-planar sites, the z -axis is taken perpendicular to the CuL_4 square planes made up of the four equatorial ligands L . In discussing whether the preferred spin orientation is along the z -axis (i.e., the easy-axis anisotropy) or in the xy -plane (i.e., the easy-plane anisotropy), the second term of Eq. (S2) is negligible compared with the first term, and the sign of A of the first term determines the anisotropy (namely, $A < 0$ for the easy-axis anisotropy, and $A > 0$ for the easy-plane anisotropy). This justifies our use of the simplified SIA expression in Eq. (2c).

References

1. (a) A. Carrington and A. D. McLachlan, *Introduction to Magnetic Resonance with Applications to Chemistry and Chemical Physics*, Harper and Row, New York, 1967. (b) A. D. McLachlan, *Mol. Phys.* **6**, 441 (1963). (c) A. Abragam and M. H. L. Pryce, *Proc. Roy. Soc. London Ser. A*, **206**, 135 (1951). (d) J. H. Van Vleck, *Rev. Mod. Phys.* **23**, 213 (1951).
2. (a) R. Maurice, P. Verma, J. M. Zadrozny, S. J. Luo, J. Borycz, J. R. Long, D. G. Truhlar, and L. Gagliardi, *Inorg. Chem.* **52**, 9379 (2013). (b) R. Maurice, R. Bastardis, C. de Graaf, N. Suaud,

- T. Mallah, N. Guihéry, J. Chem. Theory Comput. **5**, 2977 (2009). (c) R. Maurice, C. de Graaf and N. Guihéry, J. Chem. Phys. **133**, 084307 (2010).
3. D. Dai, H. J. Xiang and M.-H. Whangbo, J. Comput. Chem. **29**, 2187 (2008).

2. Supplementary figures

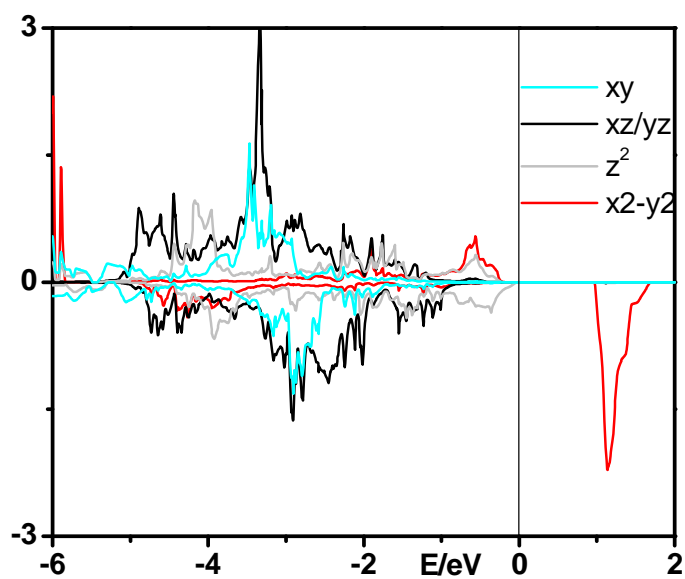


Figure S1. PDOS plots calculated for LiCuVO_4 .

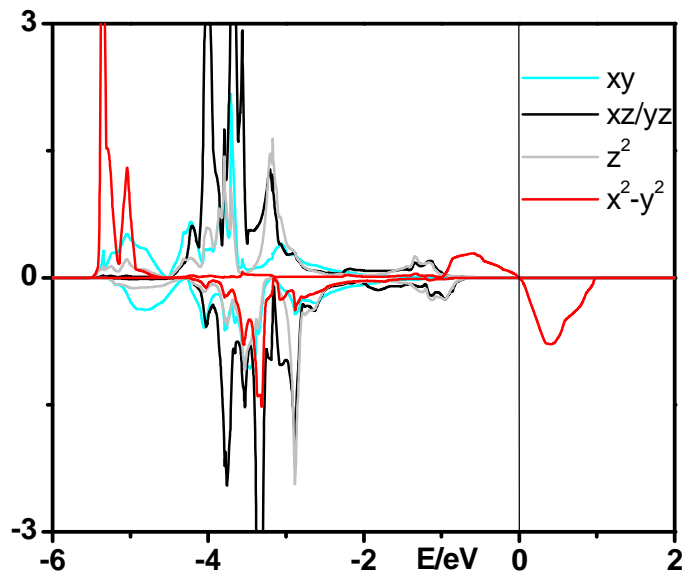


Figure S2. PDOS plots calculated for CuBr_2 .